Chapter 6

Anodic Nanostructures for Solar Cell Applications

Jia Lin, Xiaolin Liu, Shu Zhu and Xianfeng Chen

Additional information is available at the end of the chapter

http://dx.doi.org/10.5772/62396

Abstract

As a versatile, straightforward, and cost-effective strategy for the synthesis of self-organized nanomaterials, electrochemical anodization is nowadays frequently used to synthesize anodic metal oxide nanostructures for various solar cell applications. This chapter mainly discusses the synthesis of various anodic TiO_2 nanostructures on foils and as membranes or powders, and their potential use as the photoanode materials based on foils, transparent conductive oxide substrates, and flexible substrates in dye-sensitized solar cell applications, acting as dye-loading frames, light-harvesting enhancement assembly, and electron transport medium. Through the control and modulation of the electrical and chemical parameters of electrochemical anodization process, such as applied voltages, currents, bath temperatures, electrolyte composition, or post-treatments, anodic nanostructures with controllable structures and geometries and unique optical, electronic, and photoelectric properties in solar cell applications can be obtained. Compared with other types of nanostructures, there are several major advantages for anodic nanostructures to be used in solar cells. They are (1) optimized solar cell configuration to achieve efficient light utilization; (2) easy fabrication of large size nanostructures to enhance light scattering; (3) precise modulation of the electrochemical processes to realize periodic nanostructured geometry with excellent optical properties; (4) unidirectional electron transport pathways with suppressed charge recombination; and (5) large surface areas by modification of nanostructures. Due to the simple fabrication processes and unique properties, the anodic nanostructures will have a fascinating future to boost the solar cell performances.

Keywords: anodic nanostructures, membranes, scattering, photonic crystals, thermal stability, surface area

1. Introduction

1.1. Anodic oxides

The electrochemical anodization of anodic oxides is conducted with two-electrode or three-electrode configurations in an electrochemical cell, with the targeted metals as the working electrode (anode) and usually Pt/carbon as the counter electrode (cathode). The electrolytes used are typically fluoride-containing organic or aqueous solutions. A voltage is applied between the two electrodes to fabricate various nanostructures on the anodic metal surface. The anodic oxides feature the self-organized configurations with regular and open structures, such as tubes, pores, channels, bundles, powders, and various tailored shapes. The formation mechanism of oxide nanostructures is of great concern. For tube arrays, the possible processes are as follows: (1) The first step is the tube initiation. The tube growth initiates at some preferable positions on the metal surface that can provide both high local electric field and narrow channel-like surface morphology. It has been indicated that the morphological instability of the initial oxide surface layer causes the formation of pores [1]. Hence the surface state of the starting metal substrate can significantly influence the surface morphology of the anodic oxides, such as pore size distribution, regularity, and shapes. (2) The second step is the tube growth. One most accepted view is that the oxidation of the metal with the assistance of electric field forms a compact thin oxide layer (barrier layer) on the surface [2]. The thin oxide layer is also partially dissolved under the assistance of electric field. The oxidation and dissolution happen simultaneously. When the oxide growth rate at the metal/oxide interface equals to the oxide dissolution at the oxide/electrolyte interface, the thickness of the compact oxide layer keeps unchanged. Then the compact layer at the oxide/metal interface moves towards the inner part of the metals and the oxide nanostructures form into the metals.

Due the advantages such as simplicity, high efficiency, and low cost of electrochemical anodization, it has been utilized to fabricate various wide band gap metal oxide nanostructures, such as titanium oxide (TiO_2), aluminum oxide (Al_2O_3), hafnium oxide, zirconium oxide, niobium oxide, tantalum oxide, tungsten oxide, and their alloys. Among them, the most widely studied anodic oxides are Al_2O_3 and TiO_2. For Al_2O_3, usually nanoporous structures can be obtained, which can be used as filters and templates. TiO_2 nanotube structure was first reported by Zwilling in 1999 by electrochemical anodization of Ti metal in aqueous fluoride containing electrolyte [3, 4]. Recent studies have indicated that the nanotube morphology is in fact converted from nanopores by dissolution of the oxides at the interpore region. Due to the unique properties, TiO_2 nanotubes have been utilized in dye-sensitized solar cells (DSSCs), perovskite solar cells, quantum dot solar cells, photocatalysis, batteries, supercapacitors, electrochromic devices, sensors, drug release, and cell differentiation applications. In this chapter, we mainly discuss the fabrication of TiO_2 nanotubes and the design and improvement of DSSCs.

The electrochemical anodization is a highly controllable technique. The growth of anodic TiO_2 nanostructures can be influenced by many key anodization parameters, such as applied voltages, currents, bath temperatures, post treatments, and kinds of electrolyte. The

control of the complex oxidation formation and chemical etching of the oxides can be realized during the anodization process, to establish the balance between the oxidation and dissolution. As a result, the morphology, regularity, growth rate, size, length, wall smoothness, and single or double walled nanotubes can be artificially designed. For example, fast growth of nanotubes can be realized in an electrolyte-containing lactic acid, which is desirable for industry production [5]. The nanotubes with lengths ranged from several 100 nm to 1000 μm have been fabricated [6]. Furthermore, by in-situ doping with various non-metal or metal elements in the electrolytes containing additives, visible light response of the anodic oxides can be obtained. The control of anodic nanostructures will greatly influence their physical and chemical properties, and their performances in various devices.

1.2. Solar cell applications

The development of low-cost new-generation solar cells has attained broad attention recently. Dye-sensitized solar cell (DSSC) is a kind of photoelectrochemical cell with the advantages of low cost, simple synthesis, large area, and high stability. Since the first report by O'regan and Grätzel with 7.1% efficiency [7], the highest efficiency of above 13% has been achieved [8]. In DSSCs, typically TiO_2 nanoparticles are used as the photoanode material, which are coated on transparent conductive oxide (TCO) substrates to form porous networks. The dye sensitizers are adsorbed on the surface of nanoparticles to harvest incident light. The dyes are surrounded by liquid redox electrolytes, which can reduce the oxidized dyes and accept electrons from the counter electrode. In the photon-to-electricity conversion process, the light absorption and the charge transport are two separate processes. The electron-hole pairs are separated by the heterojunctions with different work functions. No obvious built-in electric field exists in DSSCs, and the electrons go through the TiO_2 network by diffusion. Inspired by the development of DSSCs, other types of sensitized solar cells such as quantum dot (QD)/semiconductor sensitized solar cells and perovskite solar cells have been introduced. For QD systems, by adjusting the size of QDs, the band gaps can be tuned [9]. Furthermore, by using QDs, multiple exciton generation effect exists [10]. The perovskite solar cells are a new type of solar cell devices. Due to the high absorption efficiency and broad absorption range of perovskite materials, the efficiency has been above 20% recently [11].

For solar cell applications, the anodic nanostructured materials are usually used to replace TiO_2 nanoparticles to fabricate the photoanodes. In DSSCs, the photoanodes mainly play two important roles. First, the nanostructures provide large specific internal surface areas for the anchoring of dyes. Second, the nanostructures provide the charge diffusion pathways to transport the injected charges to the outer circuit. As a result, the morphology, structure, crystal structure, and surface state of anodic nanostructures can determine the performance of DSSCs based on these photoanodes, including loading of dyes, light harvesting, charge transport, recombination, and collection, and finally power conversion efficiency.

2. Solar cell configuration

2.1. 1D TiO_2 nanotubes

The nanoparticle photoanodes in DSSCs have the randomly distributed sizes, and loosely and irregularly packed structures. As a result, the injected electrons encounter a large amount of nanoparticles (about 10^3 to 10^6 as estimated) when diffuse through the photoanodes. The real path for electrons to travel before reaching the substrate is very long. This increases the probability of electron recombination loss at the oxide/electrolyte interface. One-dimensional (1D) nanostructures, such as nanotubes, nanowires, nanofibers, and nanorods, can provide the directional electron diffusion, which shortens the electron pathways, and are proved to have better collection efficiency [12]. By electrochemical anodization, various 1D nanostructures have been developed, and one very important nanostructure is TiO_2 nanotubes. The first attempt to use TiO_2 nanotubes to replace nanoparticles in DSSCs is reported by Schmuki et al. [13], and afterwards various reports have been emerging. The electron recombination rate in TiO_2 nanotubes is found to be very slow, with much larger electron lifetime (more than 10 times) than TiO_2 nanoparticles [14]. Thus, anodic TiO_2 nanotubes are very promising for high performance solar cells.

2.2. Free-standing membranes

Usually, the anodic nanotubes are grown on the Ti metal foil substrate, which is opaque. When directly utilizing TiO_2 nanotubes on foils in DSSCs, back-side illumination cell configuration is needed [15]. That is to say, the solar light enters the solar cell from the counter electrode. As a result, the light would be reflected by counter electrode that is coated with a thin layer of catalyst, and also be absorbed by dark redox electrolyte before it can be absorbed by dyes loaded on the anodic nanostructures. It has been estimated that about approximately 30–40% light energy would be lost by using this back-side illumination configuration [16]. To realize the front-side light illumination and to fabricate transparent electrode for broad applications, the anodic TiO_2 nanotubes should be fabricated on the TCO substrates.

One strategy is the direct growth of TiO_2 nanotubes by anodizing the sputtered or thermal evaporated thick Ti metal films on TCO substrates. However, there exist two problems. One is that the synthesis of thick and high-quality metal films on TCO substrate is very difficult, with complex and expensive procedures. The other is that the anodization oxidation process would lead to the increase of the TCO substrate resistance, the weak connection between the anodic oxide films and the substrate, and even the peeling off of the oxide films from the substrate. The low electric conductivity will result in the efficiency loss of solar cells.

The more promising method is to peel the anodic oxide layer off the metal substrate to obtain free-standing membranes, and transfer them onto TCO substrate. Various strategies such as ultrasonication separation, solvent evaporation, selective metal dissolution, and chemical-assisted separation have been proposed to peel off the films, but the procedure is complex and need careful handling. Furthermore, to obtain open bottom structure for effective tube filling

http://dx.doi.org/10.5772/62396

and flow through application, usually additional chemical etching steps of tube bottoms are needed.

To obtain high-quality free-standing membranes with simple synthesis procedures and tunable bottom morphologies, the self-detaching method has been proposed [17]. The as-formed anodic oxide layer is thermally treated at a certain temperature, and anodized again in the same electrolyte. After a short time, the oxide layer can be peeled off from the substrate without any post-treatment procedure. If the as-formed oxide layer is subjected to heat treatment at a low temperature (e.g., 200°C), the detached layer is amorphous and shows a black color. After annealing, the layer becomes crystallized and transparent (**Figure 1a**). For high temperature-treated layer (e.g., 400°C), the tubes are crystallized in the anatase phase before detachment. As a result, the detached layer is already transparent without subsequent annealing (**Figure 1b**). The detachment is probably because of the difference in mechanical and chemical stability between the top anodic layer (which we try to peel off) and the newly formed layer underneath the top layer [18]. Furthermore, according to the heat treatment temperatures during the detachment, the free-standing oxide layer can have open tube bottoms (200°C, **Figure 1c-f**) or closed bottom ends (400°C). It should also be noted that during the detaching anodization, elevating the bath temperature can facilitate the layer detachment and promote the formation of open bottoms. This elevated temperature can reduce the electrolyte viscosity and enhance the filed-assisted chemical dissolution at the tube bottom. Also, the strategy is a green technology without the use of corrosive solution and ensures continuous production [19].

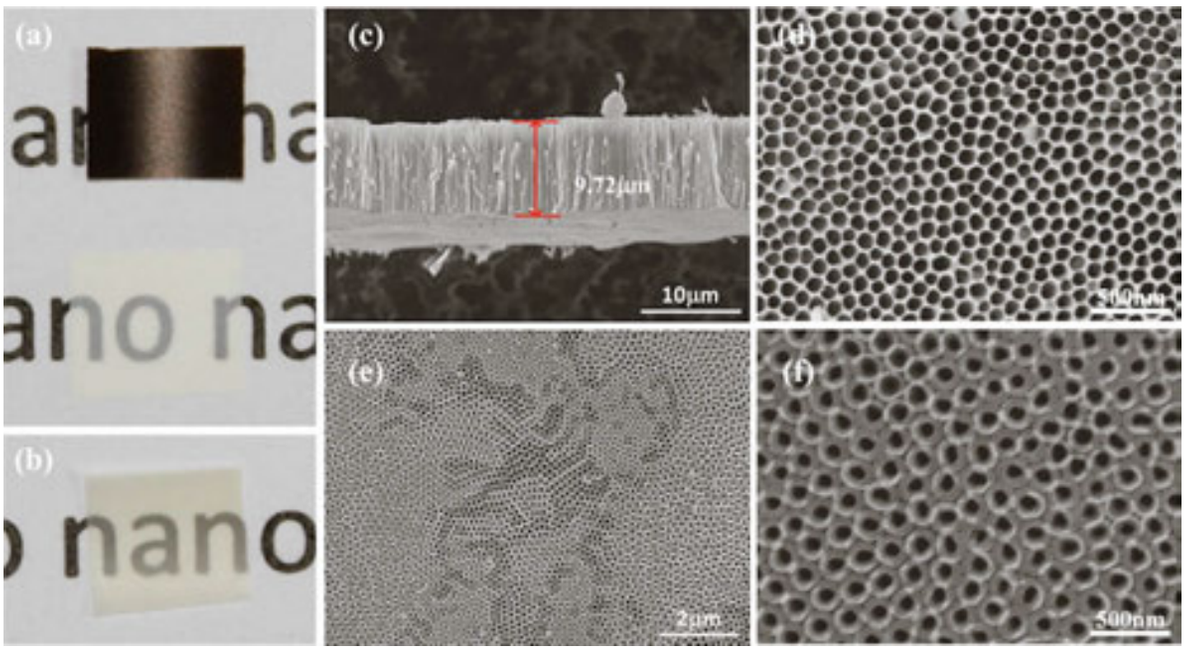

Figure 1. The photographs of (a) the detached 200°C-treated oxide layer with open bottoms before and after annealing and (b) the detached 400°C-treated oxide layer with closed bottoms. SEM images of the detached 200°C-treated oxide layer with (c) the cross-sectional view, (d) the top view, (e) the bottom view showing the open morphology, and (f) the enlarged bottom view. Reprinted with permission from Lin et al. [17].

2.3. Front-side illumination

The above-mentioned detached free-standing membranes can be used in DSSCs to achieve front-side illumination solar cell configuration, improving the light utilization efficiency. The detached oxide layer is transferred and adhered onto the TCO substrate by a thin layer of TiO_2 nanoparticles, and then sintered to enhance the connectivity (**Figure 2a**). For this detaching and transfer method, the solar cell efficiency is much higher (about 1.75 times) than on foil, due to the improvement of illumination configuration [20]. Furthermore, it has been found that tube bottom morphology also affects the solar cell efficiency. The solar cell based on tubes with open bottoms shows a better performance than that with closed bottoms, with an efficiency improvement of 17.7%. The photographs of the two kinds of photoanodes before annealing can be seen in **Figure 2b**. The removal of the tube bottom and the barrier layer can induce more dye loading of the tubes and less light scattering of the bottom caps. Furthermore, the open bottoms can facilitate the diffusion of redox electrolyte and thus reduce the recombination probability of electrons with the oxidized ions in the electrolyte [21]. Other solar cell configurations utilizing detached membranes include the bottom down or bottom-up structures and combination of nanoparticle/nanotube layers, which can be designed as required. Besides the free-standing films, nanotube powders can also be used to achieve the front-side illumination configuration, which is discussed in Section 3.

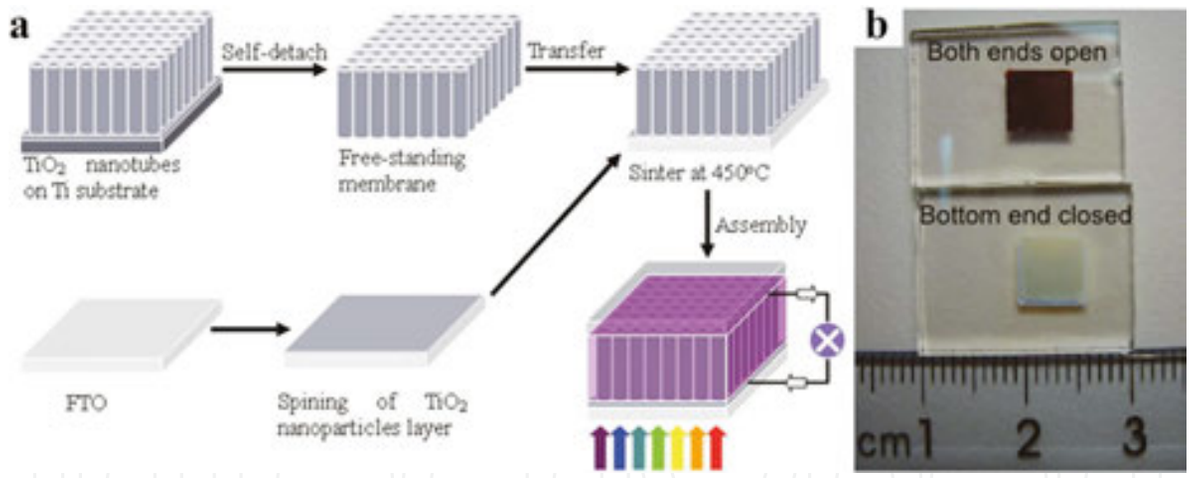

Figure 2. (a) Scheme of the fabrication procedure of front-side illuminated DSSCs using detached nanotube layers. (b) The photographs of the oxide layers with open and closed bottoms adhered onto FTO substrates. Reprinted with permission from Lin et al. [20].

3. Light scattering

3.1. Scattering effect

The widely used dyes in DSSCs commonly have high absorption efficiencies only within a narrow wavelength region, with low response for the red- and near-infrared light. Simply

http://dx.doi.org/10.5772/62396

increasing the thickness of photoelectrode film to enhance the absorption of photons will cause the increase of resistance and recombination loss. Therefore, it is essential to develop light scattering structures to increase the photon absorption opportunity by dye molecules in the weak absorption regions. As a common optical phenomenon, light scattering effect could extend the optical traveling length of incident light, so as to improve the light-harvesting efficiency and to achieve high performances. Based on Mie theory, to achieve efficient light scattering, the size of scattering centers should be comparable to the wavelength of the incident light. As a consequence, scattering structures with various morphologies have been introduced.

In general, there are three different photoelectrode configurations to combine light scattering centers. The first one is the mixed structure, for which large particles such as scattering centers are embedded into the photoelectrode films (**Figure 3a**). The scattering centers in such structure could introduce multiple scattering in the light absorption layer. However, the large particles would unavoidably cause the loss of dye adsorption because of the low surface area. The second one is the double layered structure, for which the light scattering layer is placed on the top of the nanocrystalline film (**Figure 3b**). Adding the scattering layer on the top could ensure sufficient dye loading. However, the light scattering would be weaker than in the mixed structure. The third one is the photoelectrode composed of hierarchical nanostructures with dual functions (**Figure 3c**). There have been many studies on the fabrication of such hierarchical nanocrystallite aggregates. The intensive light scattering could be guaranteed without much loss of specific surface area, but the preparation process is much more complicated. As a result, to achieve prominent light scattering and thus high DSSC performance, we should overcome the drawbacks of these structures.

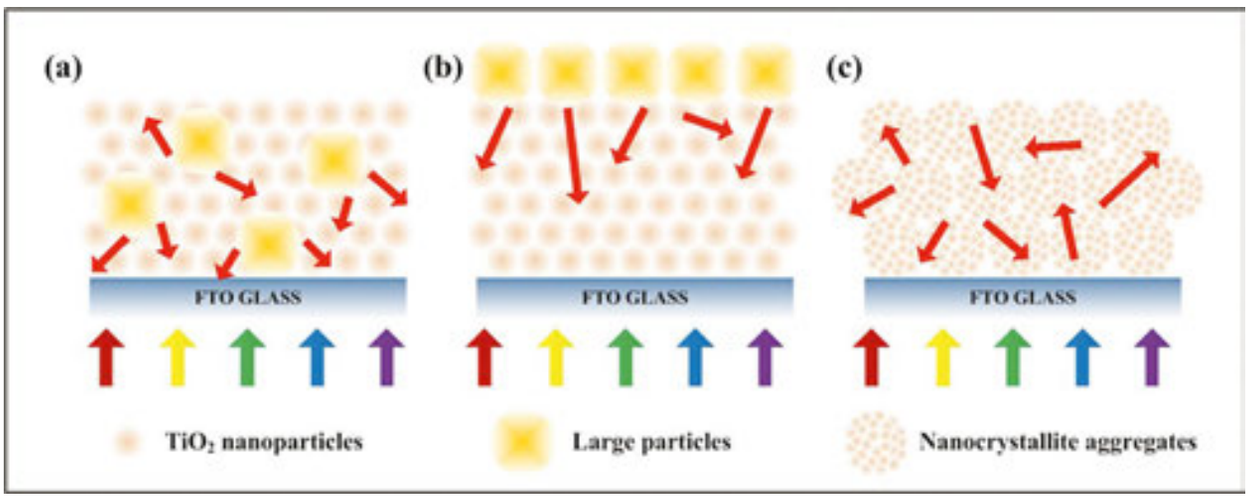

Figure 3. The schematic and light chart of the light scattering structures.

3.2. Conventional scattering centers

The large TiO_2 particles with diameters of about 200–400 nm are commonly used as light scattering centers, which can be simply mixed into the photoelectrode films to increase the light harvesting efficiency. In the early studies, Grätzel et al. have found that when TiO_2 nanoparticles are hydrothermally prepared at 250°C (normally below 230°C), the nanoparticle film would become translucent because of the spontaneous particle agglomeration [22]. Subsequently, the fabrication of large TiO_2 particles with high crystallinity has been paid more and more attention.

Besides nanoparticles, solid spheres fabricated by facile hydrothermal method also exhibit light scattering effect. However, the large particles or spheres usually suffer from low surface area for dye loading, which would affect the light harvesting. To overcome the weakness of low surface area, TiO_2 spheres with rough surfaces have been synthesized. Also, mesoporous spheres with dual functions have been fabricated by nanocrystallite clustering, which are dominant in light scattering without the loss of surface area for dye-uptake. The hollow spheres are an alternative candidate for light scattering centers because of their larger surface area and better infiltration of electrolyte. Recently, core-shell microspheres have gradually emerged and become very promising scattering center. The core-shell structure could not only provide large light scattering, but also confine the light inside the spheres.

3.3. TiO_2 nanotubes powders

Apart from the above structures, 1D nanostructures could also serve as light scattering centers, such as nanorods, nanofibers, nanotubes, and their aggregates. For example, the light-to-electricity conversion yield of 6.08% has been achieved by blending of large TiO_2 nanorods (800 nm) and small nanorods (20–40 nm) on the top of small nanorod films, benefit from the low charge transport resistance and high light scattering effect [23]. TiO_2 nanofibers have been readily fabricated by simple electrospinning and applied in DSSCs as photoanode films [24]. The mixture of 1D nanostructures with nanoparticles could make a significant improvement of the performance of DSSCs also because of the combined effect of strong light scattering, abundant dye-loading amounts, and the improvement of electron transport properties.

TiO_2 nanotube arrays with 1D nanostructure have been found to have prominent light scattering effect, with the combination of superior electron transport when applied in DSSCs [14, 25]. Due to the formation of large crystalline grains and existence of nanotube bundles, the TiO_2 nanotubes could generate effective light scattering. Lee et al. [26] obtained TiO_2 nanotube powders and coated the powders on the top of the nanocrystalline film, and attained noticeable increment of light harvesting.

The mixed structures of nanotubes and nanoparticles have also been explored in many studies. Embedding nanotube powders inside the nanoparticle film can (1) promote the permeation of liquid electrolyte, (2) increase the electron transport in the photoanode, and (3) introduce the scattering effect of nanotubes, which would be profitable for high perform-

http://dx.doi.org/10.5772/62396

ance DSSCs. Lin et al. have fabricated TiO_2 nanotubes by anodic growth and involved ultrasonic separation of the resulted nanotubes to obtain TiO_2 nanotube powders (**Figure 4a**) [27]. To reduce the electron trap states, the nanotube powders are thermally treated at a high annealing temperature (650°C) to enhance crystallinity (the details are discussed in Section 5). The hybrid photoanodes can be formed by mixing these highly crystallized nanotube powders with TiO_2 nanoparticles (**Figure 4b**). By adjusting the weight ratio of the nanotube powders, the performance of DSSCs could be optimized and the highest efficiency of 6% has been achieved.

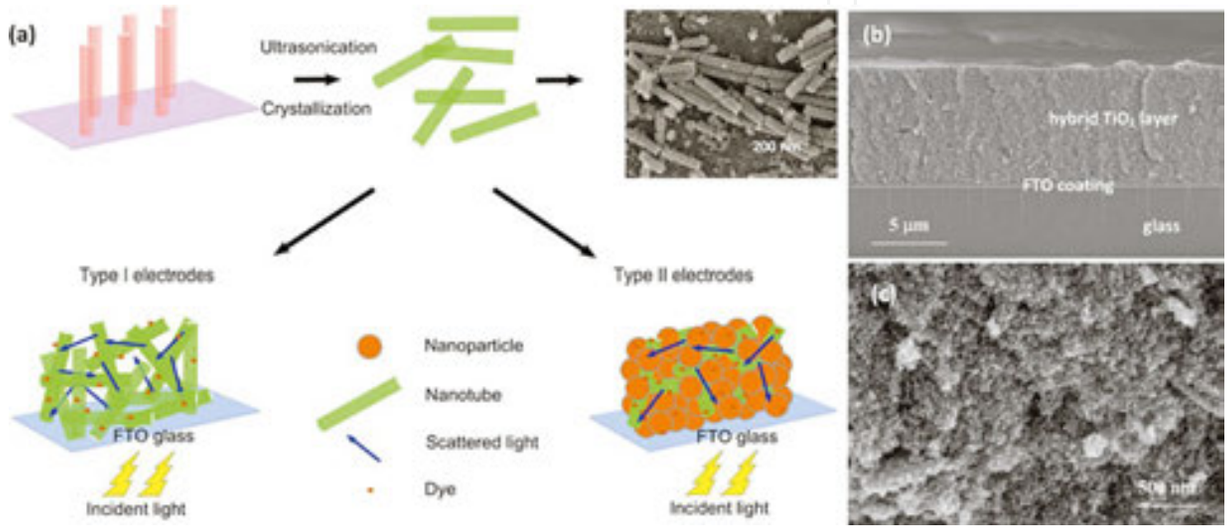

Figure 4. The schematic of the fabrication procedures of nanotube powders, nanotube electrode, and hybrid electrode. (b, c) The cross-sectional views of the hybrid photoanode with nanotubes embedded in nanoparticles. Reprinted with permission from Lin et al. [27].

3.4. Large nanotubes

Generally, the diameter of nanotubes fabricated by conventional electrochemical anodization is about 100 nm, which is obviously smaller than the wavelength of visible light. The large diameter nanotubes of size comparable to the visible light wavelength (500 nm or above) can be synthesized under high-voltage anodization. For example, by anodization at a high voltage of 180 V in an organic electrolyte containing lactic acid (aged for 10 hours), large nanotubes with top diameter of 300 nm and bottom diameter of 500 nm have been fabricated (**Figure 5a,b**) [28]. The resulting nanotube membranes are transferred onto a thick TiO_2 nanocrystalline film to act as the light scattering layer (**Figure 5c,d**). The large diameter nanotubes show a superior scattering property, and the photoanode incorporated with large nanotubes on top is nearly opaque in visible light (**Figure 5e**). By introducing the large diameter nanotube membranes, the performance of DSSCs has been greatly improved, which is 19% higher than that without scattering layer, and 11% higher than that using normal nanotubes (100 nm) as the scattering layer (**Figure 5f**).

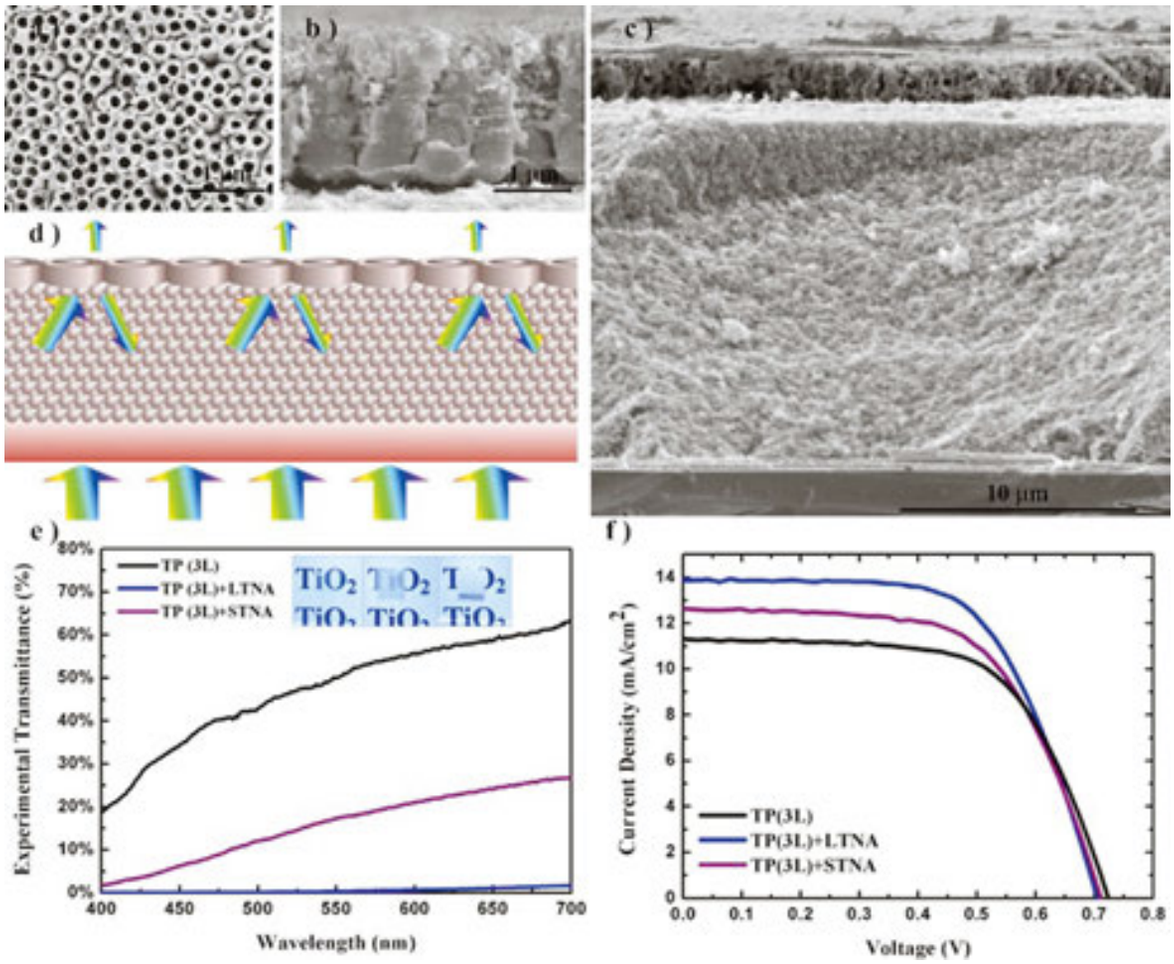

Figure 5. SEM images of large diameter nanotubes with (a) the top view and (b) the cross-sectional view. (c) SEM image and (d) schematic of double-layered photoanode using large nanotubes as the scattering layer. (e) The transmittance spectra of the photoanodes without scattering layer (TP(3L)), with normal nanotubes (TP(3L) + STNA), and with large nanotubes (TP(3L) + LTNA) as scattering layers. (f) Photocurrent-voltage curves of the DSSCs based on these photoanodes. Reprinted with permission from Liu et al. [28].

To enhance the functionality of the photoanodes of DSSCs, the multi-stacked photoanodes have also been developed by integration of three or more various TiO_2 architectures [29, 30]. For TiO_2 nanotubes, the similar multi-layered structures have been fabricated (**Figure 6a**), based on the study of large diameter nanotubes [31]. First, bi-layered TiO_2 nanotube membrane with top large nanotubes (~540 nm) and underlayer normal nanotubes (~130 nm) has been fabricated by two-step anodization in different kinds of electrolytes (**Figure 6b**). Secondly, the bi-layered membrane is transferred onto a layer of TiO_2 nanoparticles for building photoanodes. The three layers are stacked together with gradually decreased sizes from top to bottom. For this type of multi-layered photoelectrode, layers with different tailored nanostructures play different roles on the performance of the DSSCs. By optimizing the thickness and synergistic effects of each layer (**Figure 6c**), large amounts of dye adsorption, reduced recombination during the electron diffusion, and efficient light scattering can be simultaneously guaranteed. DSSCs based on the multi-functional photoanode shows a photoelectric efficiency as high as 6.52%.

http://dx.doi.org/10.5772/62396

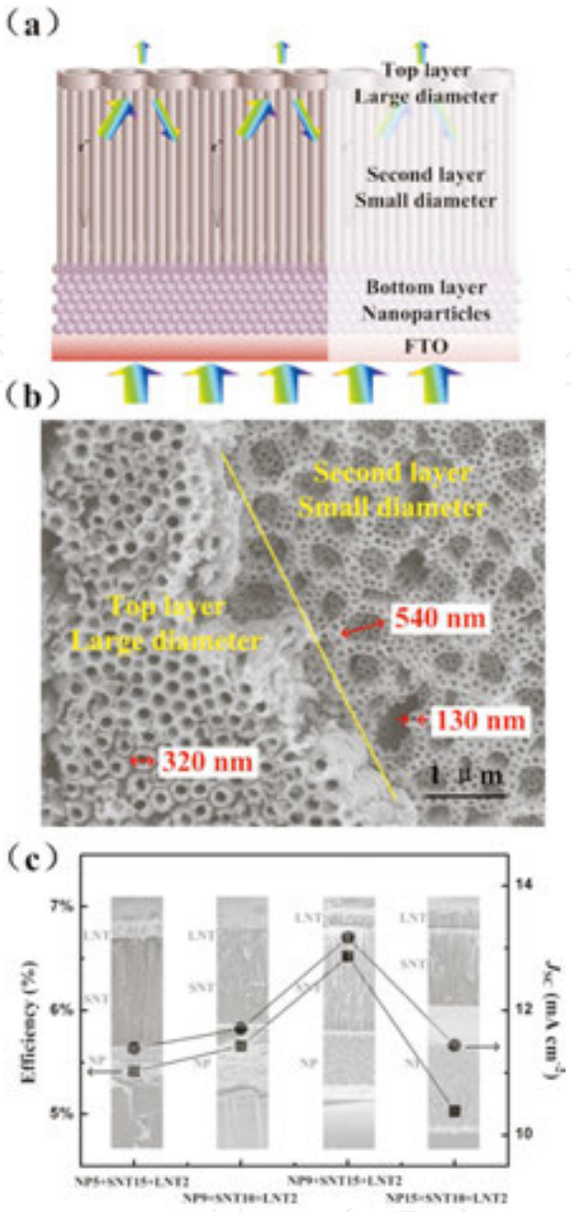

Figure 6. (a) The schematic of the multi-layered photoanode with top layer large diameter nanotubes (LNT), second layer normal nanotubes (SNT), and bottom layer nanoparticles (NP). (b) SEM image of the bilayered nanotube membrane. (c) The solar cell efficiencies based on multi-layered photoanodes with different layer thicknesses. Reprinted with permission from Liu et al. [31].

4. Photonic crystal structures

4.1. Photonic crystal effect

As illustrated above, the improvement of light harvesting is very important to enhance the solar cell performances. Besides light scattering centers, the photonic crystals (PCs), including one-dimensional (1D), two-dimensional (2D), and three-dimensional (3D) structures, can also

be used to enhance the light harvesting. PCs are the optical materials with periodically changed refractive index. By adding PCs on the top of nanocrystalline film, PCs will greatly influence the light behavior inside the photoanode, to reflect the light, which would transmit through the photoanode back to the photoanode if the light is in the band gap of PCs, reabsorbed by dye molecules. The possible mechanisms of PC effect are photon localization, special photon behavior at the band edge, and light reflection.

The PC structures can be fabricated by various strategies, such as self-assembly, lithography, and laser writing. For example, TiO_2–SiO_2 nanoparticle alternate layers have been deposited onto TiO_2 nanoparticle mesoporous layer by spin-coating to act as 1D PCs [32]. The fabrication of such multi-layers, however, needs complex processing procedures. Using soft-lithographic technique, 2D PCs with high periodicity have been produced, to enhance the photocurrent generation in DSSCs [33]. 3D PCs usually consist of opal/inverse opal structures from PS spheres [34–36], which can provide a complete photonic band gap and large enhancement in light harvesting.

4.2. Anodic photonic crystals

For PC applications, the excellent regularity of anodic nanostructures is required. The porous and tube structures by electrochemical anodization have the inherent 2D periodicity. Due to the high periodicity, porous Al_2O_3 nanostructures have been applied as 2D PCs for applications such as lasing and light-emitting diode [37, 38]. However, for TiO_2 nanotubes, due to the randomness of tube initiation, the regularity is not so satisfactory. To obtain highly ordered arrays, focused ion beam (FIB) sculpting has been used to achieve the patterned metal surface prior to anodization, which can guide the subsequent nanotube growth. This technique has been largely studied by Lu et al. [39], both on Ti and Al metals, and various kinds of patterns have been produced. The regularity can well meet the requirement of PCs, but the main problem is that the fabrication procedure is complex and time-consuming, which is not suitable for large-scale production. By using the so-called two-step or multi-step anodization [40], the dips formed by the first-step anodization on the metal surface can also act as the template to guide the tube growth, improving the tube regularity to a certain extent.

4.3. TiO_2 nanotube 3D photonic crystals

Usually, the anodized TiO_2 nanotubes have the smooth tube walls (**Figure 7a**). By the constant voltage anodization in certain electrolytes, the random and spontaneous current oscillation can lead to the formation of small ripples on the tube walls (**Figure 7b**). Inspired by this phenomenon, the fabrication of regular 1D nanostructures along the tube axis has been proposed. For Al_2O_3, Lee et al. [41, 42] tried to fabricate 3D ordered nanoporous structure by mild and hard anodization in two different electrolytes. Periodic voltage anodization (cyclic anodization or pulse voltage anodization) has also been used to fabricate branched nanostructures for PCs [43]. The key point to induce the structure change along the longitudinal direction is the abruption of the established steady growth state of anodic nanostructures. TiO_2 possesses higher refractive index ($n \sim 2.7$) than Al_2O_3 ($n \sim 1.7$), more suitable to be used as structural color materials to realize the complete bandgap. Hence, the strategies to induce ordered periodic

http://dx.doi.org/10.5772/62396

structure along the TiO_2 tube axis have been greatly concerned. The bamboo-type TiO_2 nanotubes have been achieved by the periodic or pulse voltage anodization [44], which have certain longitudinal periodicity. However, due to the unstable nanotube growth rate under constant voltage anodization, the periodic voltage can only fabricate the structures with short range regularity. Furthermore, the structural parameters and thus PC characteristics cannot be preciously adjusted.

To realize the strict control of regularity, the periodic structures along the longitudinal direction can be fabricated by periodic current anodization [45]. Because the applied current is directly related to the growth rate of anodic oxide, the steady current can ensure the uniformity of the oxide growth and the control of the interrupt of current can lead to the periodic structures along the axis. During the current pause, the oxide growth stops, but the chemical dissolution continues, resulting in the structural difference on the tube walls (**Figure 7c**). Unlike the smooth or rippled tube wall morphologies, the tube segments can be clearly observed with the concave shaped interfaces. In the range of about 20 periods from top to bottom, the distance between segments (period length) is almost the same, revealing excellent long-range regularity (**Figure 7d**).

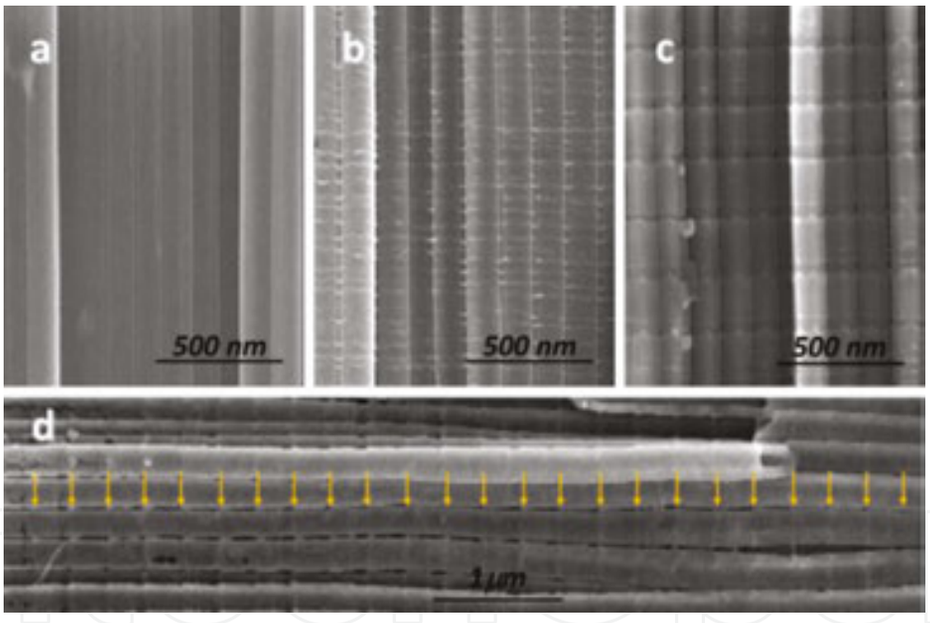

Figure 7. The cross-sectional SEM image of the periodic structures with (a) smooth, (b) rippled, and (c) periodic tubes with concave interfacial morphologies. (d) The periodic structures along the tube axis with long-range regularity (period length: 292 nm). Reprinted with permission from Lin et al. [45].

As discussed above, due to the higher reflective index, TiO_2 is more suitable photonic material than Al_2O_3. By using periodic current-pulse sequences, the photonic features of TiO_2 nanotubes, including period length, interfacial morphology, period number, and type of period (periodic, quasiperiodic, or aperiodic), can be precisely and continuously modulated by the anodization parameters. The periodic nanotube films (after detachment) with different period lengths show different colors and transparencies (**Figure 8a**), and corresponding different

reflection spectra (**Figure 8b**). Furthermore, the structural color of the nanostructured film is not static. The film with fixed period structure shows different colors with different light incident and viewing angles (**Figure 8c**).

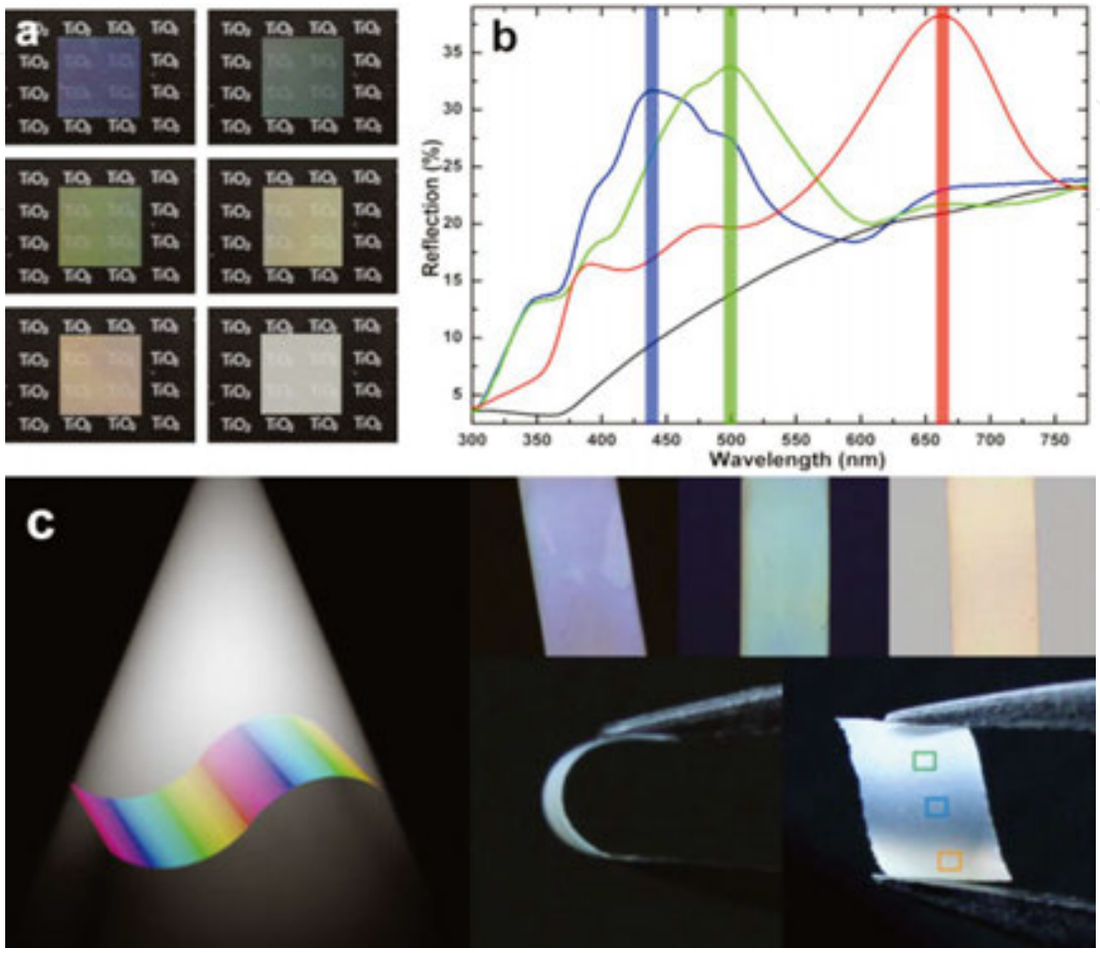

Figure 8. The optical images of the colorful films, from purple to red. (b) The reflection spectra of the colorful films, showing the bandgaps. (c) The change of film colors with different incident and viewing angles and the flexibility of the colorful films. Reprinted with permission from Lin et al. [45].

TiO_2 nanotube PCs have been coupled directly to nanotube layers in DSSCs by a single step [46]. Also the thin PC membrane can be placed on the top of nanocrystalline TiO_2 layers as semi-transparent photoanode for DSSCs [47]. During the design of the solar cells, we should consider the match between the bandgap of PC structures and the incident light spectrum, to maximize the solar cell light harvesting. Thus, the different PCs with different band structures are designed and coupled to DSSCs. When using N719 dye as light absorber, it is found that DSSCs coupled with 150 nm periodic structure show the best performance. The advantages of the strategy using the above 3D nanotube PCs in solar cells are (1) tunable photonic structure, (2) controllable fabrication process, (3) easy integration by direct fabrication of both light absorbing layer and PC layer tubes by a single-step anodization or by membrane transfer, (4) tight mechanical and electrical connection between the light absorbing layer and PC layer,

facilitating the charge transport, (5) interconnected two layers at the interface region, facilitating the electrolyte infiltration, and (6) easy fabrication of large area, transparent, and flexible PC films.

5. Electron properties

5.1. Substrate effect

In DSSCs, the widely used model describing the diffusion process in the TiO_2 electrode is the multiple trapping model. During the electron transport, the electron undergoes the trapping and detrapping processes by the trap states. To enhance the charge collection and thus efficiency, the fast transport and slow recombination of electrons are required. It has been reported that the order of the nanomaterials can greatly influence the electron property. For disordered nanoparticles, there exist numerous particle–particle interfaces. While for nanotubes, electrons transport along the tube axis, which would lead to higher electron transport rate [48, 49]. However, in anodic tubes, the transport is not as fast as expected. Various studies have been devoted to investigating the possible underlying mechanism. The widely accepted view is that there exist a large amount of trap states in tubes, as compared with nanoparticles, which suppress the electron transport [14, 50, 51]. The trap states, usually oxygen vacancies or Ti^{3+} ions, are most likely originated from non-crystallized amorphous regions, grain boundaries, and the impurities induced during the anodization process.

The improvement of tube crystallinity by high temperature annealing is supposed to be useful for the reduction of the trap densities. However, usually the substrate effect exists during annealing of anodic oxides on metal substrate. That is to say, the metal substrate can greatly affect the crystal phase and nanostructure of the oxide film layer during the annealing process. For TiO_2 nanotubes on Ti, rutile phase can be detected at a low annealing temperature of 400–450°C. Furthermore, the nanotubes are gradually condensed at high temperatures, and finally the porous structure is fully destroyed at about 700–800°C. This is due to the fact that the Ti foil can be directly oxided to the rutile phase during high temperature annealing, forming a thin and compact oxide layer at the oxide/metal interface region, and gradually becomes thicker [52]. This rutile layer will initiate the crystal phase and structure transformation of the upper TiO_2 layer, from the bottom to the top. The substrate effect exists at different annealing conditions, and even more severe when the annealing temperature increases [53–55]. Thus, anodic oxide films on metal foils can only be crystallized at a relatively low annealing temperature for DSSC applications. The high temperature annealing would cause the destruction of nanostructure and increase of resistance, both of which deteriorate the solar cell performance.

5.2. Highly crystallized nanotubes

To realize the high temperature annealing and thus highly crystallized TiO_2 nanotubes for DSSCs, the substrate effect should be eliminated. This can be realized by annealing of free-standing TiO_2 nanotube membranes before the attachment of the membrane onto the TCO

substrate. For membranes without metal substrate, the substrate effect does not exist, and the crystallization behavior is completely different. There have been several attempts to anneal membranes at high temperatures [56–58]. The initiation temperature of phase transformation and structure densification becomes much higher. The main problem is that during the high temperature annealing, the membrane is inclined to curling and cracking, due to the low quality of the membranes fabricated by various strategies. By optimizing the self-detaching anodization process as discussed in Section 2, high-quality TiO_2 nanotube membranes can be obtained. The membranes can withstand the high temperature annealing up to 700°C and the hollow, porous, and ordered structure is maintained (**Figure 9a–e**) [59], although the crystallites in the tube walls gradually become larger (**Figure 9f**).

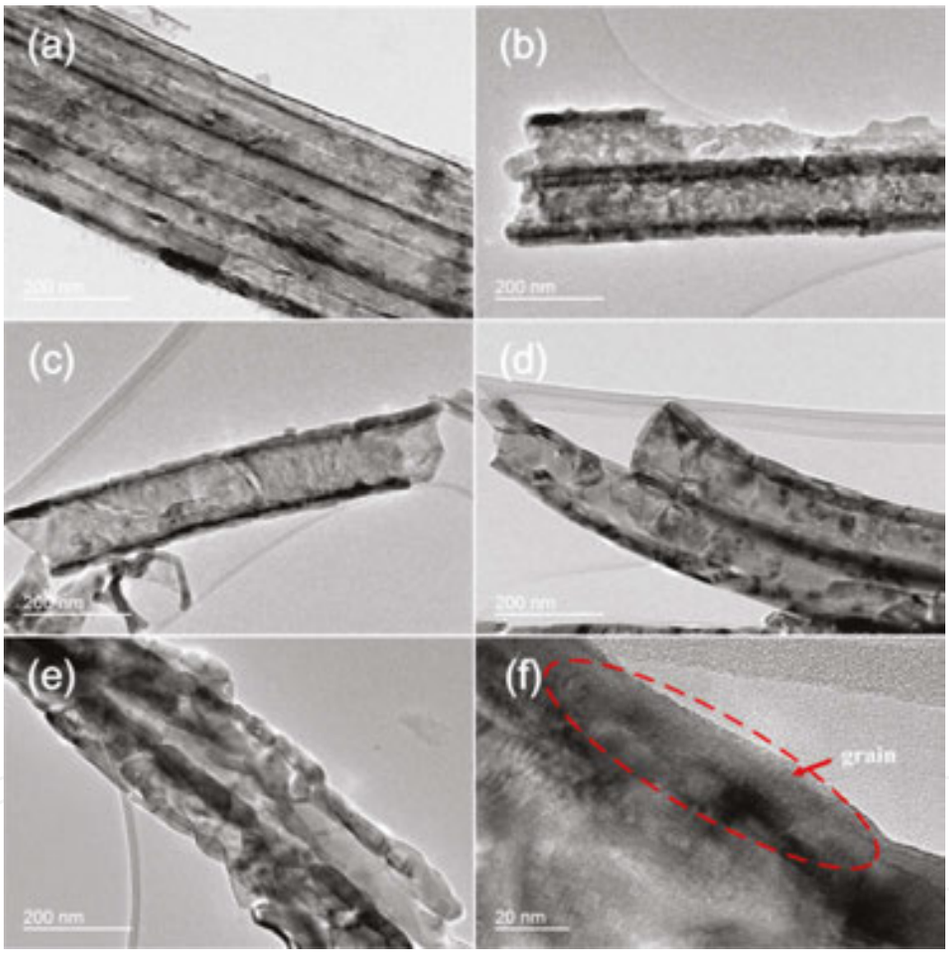

Figure 9. TEM images of tube membranes annealed at (a) 400, (b) 500, (c) 600, (d) 700, and (e) 800°C. (f) HRTEM view of the grain in the tube walls annealed at 700°C. Reprinted with permission from Lin et al. [59].

The TiO_2 nanotube membranes with high crystallinity have been used as the photoanode in DSSCs (**Figure 10a**). The electron transport is found to be enhanced significantly because of the reduction of the impurity and defects and thus the electron trap states. As a result, the electron diffusion length is much longer in the highly crystallized nanotube membranes (**Figure 10b**). Despite the lower surface area and thus lower dye loading amount, a significantly

http://dx.doi.org/10.5772/62396

improved solar cell efficiency of 7.81% has been obtained for 700°C annealed sample. The high temperature annealing for enhancement of crystallinity can also be used to fabricate flexible DSSCs. For such type of solar cells, the high temperature annealing is also not applicable because the flexible substrate (usually PET or PEN) cannot withstand high temperatures. For membranes, the high temperature annealing is completed before the transfer of nanotubes to the flexible substrate. Thus, the conductivity and quality of flexible substrate are not influenced by the high temperature annealing process. The only problem is how to keep the membrane adhered tightly to the flexible substrate, ensuring the electron transport pathways [60].

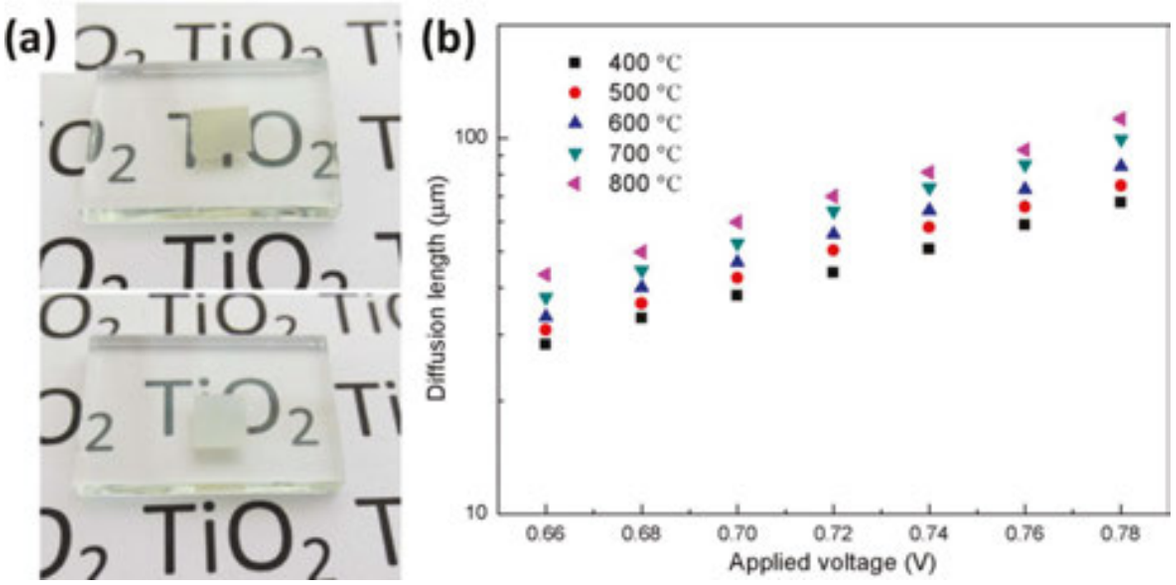

Figure 10. (a) The photographs of photoanodes consisting nanotube membranes annealed at 400 and 700°C. (b) The variation of diffusion length in DSSCs as a function of annealing temperature. Reprinted with permission from Lin et al. [59].

6. Surface areas

6.1. Small size nanotubes

Anodic TiO_2 nanotubes usually have low specific surface areas (BET surface area ~20 m^2/g), as compared with other nanomaterials. For normal hexagonal closely packed nanotube arrays, due to the compact and ordered structure, large tube size, and smooth tube wall, the internal surface area is limited. When the nanotubes are applied in DSSCs as the photoanode material, the light cannot be fully absorbed, leading to low light harvesting efficiency. To increase the surface area, the most common strategy is the decoration of small diameter nanoparticle on the hollow tube inner or outer surface by $TiCl_4$ treatment or immersion filling, to fabricate tube/particle mixed structure. The synthesis of bi-layered structure consisting of both tube layer and nanoparticle layer, double-walled nanotubes, and bamboo type tubes with rings or ripples on tube outer walls are all benefit for the improvement of surface areas.

Fabrication of small diameter but large thickness tube layer is another strategy to increase the surface area. Typically the small diameter tubes are very short [61], and thus the surface area per electrode area is still very low. The attempt has been focused on the fabrication of high aspect ratio tubes with small diameters and large thicknesses, increasing the dye loading amount per electrode area. In usual anodization conditions, it has been found that the outer diameter of TiO_2 nanotubes is proportional to the anodization voltage within a certain range, but inversely proportional to the bath temperature. By anodization at a low voltage and a high temperature, the diameter can be greatly reduced. When the bath temperature increases from 20 to 50°C, the outer diameter can be decreased from 93 to 75 nm [62]. On the other hand, the high bath temperature can promote the growth of anodic nanotubes, leading to the small tubes with large thicknesses, which can provide enough surface area for dye anchoring.

6.2. Water immersion treatment

Besides the in-situ anodization strategies, post-treatment method can also be used to tune the geometry and structure of nanotubes and guarantee the sufficient surface area for dye adsorption. By simple water immersion of as-grown TiO_2 nanotubes at room temperature (about 1–3 days) or hot water immersion, the tube wall morphology can be changed in a controllable way [63]. This is only useful for as-formed tubes before annealing, which are amorphous. The water treatment leads to the formation of hybrid-walled tubes with outer wall unchanged (smooth tubes) while inner wall converted to small nanoparticles (**Figure 11a,b**). The TEM image clearly shows that in the hybrid structure, the tube outer wall consists elongurated nanocrystallites along the tube axis with lengths of dozens of nanometers to several hundred nanometers (**Figure 11c**). The small nanoparticles existing in the inner wall have the average crystal size of about 11 nm. The hybrid structure of the tube wall after water treatment appears to be similar to the filling or decoration of tube inner part with small nanoparticles. But it is apparently different than after water treatment, the solid tube wall appears to become thinner. This can be explained by the fact that in hybrid tubes, the nanoparticles in the inner wall are, in fact, converted from the tube wall. The formation of particles consumes the tube wall.

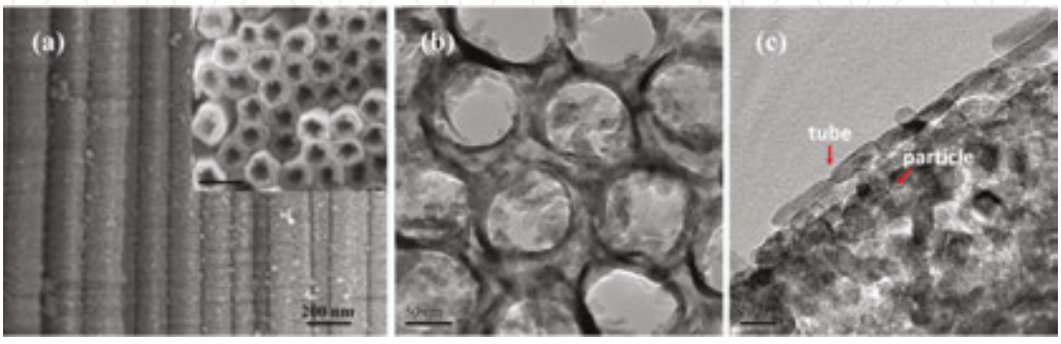

Figure 11. (a) The cross-sectional SEM images of the hybrid tubes by water immersion treatment. The insert is the top view. (b, c) TEM images of the hybrid structure consisting tubes and particles. Reprinted with permission from Lin et al. [63].

http://dx.doi.org/10.5772/62396

During the water immersion process, the inner wall is inclined to be converted to nanoparticles. Normally the tube wall fabricated in organic electrolyte consists of inner and outer shells. The inner shell contains a large amount of carbon, which is originated from the anodization electrolyte in the anodization process [64]. Due to the different chemical compositions of the two shells, the inner walls are more easily to be converted by water to nanoparticles. This is a simple but effective way to enhance the tube roughness. Also along with the structure change, partial phase transition of nanotubes from amorphous to anatase has been observed. But if the tubes are annealed (>200°C), the tubes are stable, and the water immersion cannot cause any structural change even for a long time. It has been reported that the TiO_2 dissolution/precipitate process in water would cause the rearrangement of the construction unit of TiO_2, leading to the spontaneous variation of crystal structure and morphology [65, 66].

As discussed above, the conversion of the inner tube wall to nanoparticles can enhance the tube roughness and lead to the full utilization of the tube hollow space, increasing the internal surface area of anodic nanotubes, while keeping the tubular morphology unchanged. That is to say, the unique properties of tubes can be maintained, such as more convenient dye adsorption and electrolyte infiltration, short electron diffusion path, and slow electron recombination. After the subsequent annealing, the hybrid nanostructures are applied in DSSCs. The BET surface area increases with increasing immersion time. Before treatment, the BET surface area is about 20.1 m^2/g, and increases to 39.9 and 42.7 m^2/g after 2 and 3 days immersion, respectively. The 3 days water treated sample has a BET surface area about 2.1 times larger than normal tubes. Accordingly, the photoanode dye loading amount increases by 38.9% and 57.8% as compared with normal tubes. An optimized efficiency of 6.06% is obtained, improved by about 33%. Due to the maintenance of tubular structure, the water treatments do not affect the electron recombination property. This is beneficial for the improvement of the DSSC efficiency as compared with previous report that the nanotubes decorated with nanoparticles showed decreased electron lifetimes [67, 68].

7. Conclusion remarks

This chapter discusses about the fabrication of anodic nanostructures by electrochemical anodization and their application in dye-sensitized solar cells to enhance the power conversion efficiency. The solar cell configurations can be optimized by free-standing anodic membranes to maximize the light utilization. By using large-sized nanotubes, due to the light scattering effect, the full interaction of the incident light with the absorbing layer can enhance the light harvesting of the solar cells. For periodic structures, the interface of the period is typically voids, resulting in the required periodic modulation of the refractive index for photonic crystals, which show the tunable photonic bandgaps, a property very attractive for light harvesting. By fabrication of high-quality membranes, highly crystallized nanotube membrane can be obtained, which can provide superior electron collection properties in solar cells. The surface areas of nanotubes can be increased by using high-aspect-ratio nanotubes and tube wall modification. The solar cells equipped with the proposed anodic nanostructures are expected to show excellent device performances, valuable for practical applications.

Author details

Jia Lin, Xiaolin Liu, Shu Zhu and Xianfeng Chen*

*Address all correspondence to: xfchen@sjtu.edu.cn

Shanghai Jiao Tong University, Shanghai, China

References

[1] Hebert K.R., Albu S.P., Paramasivam I., Schmuki P. Morphological instability leading to formation of porous anodic oxide films. Nature Materials. 2011; 11 (2): 162–166.

[2] Macak J., Tsuchiya H., Ghicov A., Yasuda K., Hahn R., Bauer S., et al. TiO_2 nanotubes: Self-organized electrochemical formation, properties and applications. Current Opinion in Solid State and Materials Science. 2007; 11 (1): 3–18.

[3] Zwilling V., Aucouturier M., Darque-Ceretti E. Anodic oxidation of titanium and TA6V alloy in chromic media. An electrochemical approach. Electrochimica Acta. 1999; 45 (6): 921–929.

[4] Zwilling V., Darque-Ceretti E., Boutry-Forveille A., David D., Perrin M.-Y., Aucouturier M. Structure and physicochemistry of anodic oxide films on titanium and TA6V alloy. Surface and Interface Analysis. 1999; 27 (7): 629–637.

[5] So S., Lee K., Schmuki P. Ultra-fast growth of highly ordered anodic TiO_2 nanotubes in lactic acid electrolytes. Journal of the American Chemical Society. 2012; 134 (28): 11316–11318.

[6] Paulose M., Prakasam H., Varghese O., Peng L., Popat K., Mor G., et al. TiO_2 nanotube arrays of 1000 μm length by anodization of titanium foil: Phenol red diffusion. The Journal of Physical Chemistry C. 2007; 111 (41): 14992–14997.

[7] O'regan B., Grätzel M. A low-cost, high-efficiency solar cell based on dye-sensitized colloidal TiO_2 films. Nature. 1991; 353 (6346): 737–740.

[8] Mathew S., Yella A., Gao P., Humphry-Baker R., Curchod B.F., Ashari-Astani N., et al. Dye-sensitized solar cells with 13% efficiency achieved through the molecular engineering of porphyrin sensitizers. Nature Chemistry. 2014; 6 (3): 242–247.

[9] Kongkanand A., Tvrdy K., Takechi K., Kuno M., Kamat P.V. Quantum dot solar cells. Tuning photoresponse through size and shape control of CdSe-TiO_2 architecture. Journal of the American Chemical Society. 2008; 130 (12): 4007–4015.

[10] Sambur J.B., Novet T., Parkinson B. Multiple exciton collection in a sensitized photovoltaic system. Science. 2010; 330 (6000): 63–66.

[11] Zhou H., Chen Q., Li G., Luo S., Song T.-b., Duan H.-S., et al. Interface engineering of highly efficient perovskite solar cells. Science. 2014; 345 (6196): 542–546.

[12] Law M., Greene L.E., Johnson J.C., Saykally R., Yang P. Nanowire dye-sensitized solar cells. Nature Materials. 2005; 4 (6): 455–459.

[13] Macák J.M., Tsuchiya H., Ghicov A., Schmuki P. Dye-sensitized anodic TiO_2 nanotubes. Electrochemistry Communications. 2005; 7 (11): 1133–1137.

[14] Zhu K., Neale N.R., Miedaner A., Frank A.J. Enhanced charge-collection efficiencies and light scattering in dye-sensitized solar cells using oriented TiO_2 nanotubes arrays. Nano Letters. 2007; 7 (1): 69–74.

[15] Paulose M., Shankar K., Varghese O., Mor G., Hardin B., Grimes C. Backside illuminated dye-sensitized solar cells based on titania nanotube array electrodes. Nanotechnology. 2006; 17 (5): 1446–1448.

[16] Kim J.Y., Noh J.H., Zhu K., Halverson A.F., Neale N.R., Park S., et al. General strategy for fabricating transparent TiO_2 nanotube arrays for dye-sensitized photoelectrodes: Illumination geometry and transport properties. ACS Nano. 2011; 5 (4): 2647–2656.

[17] Lin J., Chen J., Chen X. Facile fabrication of free-standing TiO_2 nanotube membranes with both ends open via self-detaching anodization. Electrochemistry Communications. 2010; 12 (8): 1062–1065.

[18] Macak J., Aldabergerova S., Ghicov A., Schmuki P. Smooth anodic TiO_2 nanotubes: annealing and structure. Physica Status Solidi (a). 2006; 203 (10): R67–R69.

[19] Wang D., Liu L. Continuous fabrication of free-standing TiO_2 nanotube array membranes with controllable morphology for depositing interdigitated heterojunctions. Chemistry of Materials. 2010; 22 (24): 6656–6664.

[20] Lin J., Chen J., Chen X. High-efficiency dye-sensitized solar cells based on robust and both-end-open TiO2 nanotube membranes. Nanoscale Research Letters. 2011; 6 DOI: 10.1186/1556-276x-6-475.

[21] Yip C.-T., Guo M., Huang H., Zhou L., Wang Y., Huang C. Open-ended TiO_2 nanotubes formed by two-step anodization and their application in dye-sensitized solar cells. Nanoscale. 2012; 4 (2): 448–450.

[22] Barbe C.J., Arendse F., Comte P., Jirousek M., Lenzmann F., Shklover V., et al. Nanocrystalline titanium oxide electrodes for photovoltaic applications. Journal of the American Ceramic Society. 1997; 80 (12): 3157–3171.

[23] Kuo P.-L., Jan T.-S., Liao C.-H., Chen C.-C., Lee K.-M. Syntheses of size-varied nanorods TiO_2 and blending effects on efficiency for dye-sensitized solar cells. Journal of Power Sources. 2013; 235: 297–302.

[24] Yang L., Leung W.W.F. Application of a bilayer TiO_2 nanofiber photoanode for optimization of dye-sensitized solar cells. Advanced Materials. 2011; 23 (39): 4559–4562.

[25] Zheng Q., Kang H., Yun J., Lee J., Park J.H., Baik S. Hierarchical Construction of self-standing anodized titania nanotube arrays and nanoparticles for efficient and cost-effective front-illuminated dye-sensitized solar cells. ACS Nano. 2011; 5 (6): 5088–5093.

[26] Lee K.S., Kwon J., Im J.H., Lee C.R., Park N.-G., Park J.H. Size-tunable, fast, and facile synthesis of titanium oxide nanotube powders for dye-sensitized solar cells. ACS Applied Materials & Interfaces. 2012; 4 (8): 4164–4168.

[27] Lin J., Zheng L., Liu X., Zhu S., Liu Y., Chen X. Assembling of a high-scattering photoelectrode using a hybrid nano-TiO_2 paste. Journal of Materials Chemistry C. 2015; 3 (26): 6645–6651.

[28] Liu X., Guo M., Cao J., Lin J., Tsang Y.H., Chen X., et al. Large-diameter titanium dioxide nanotube arrays as a scattering layer for high-efficiency dye-sensitized solar cell. Nanoscale Research Letters. 2014; 9 (1): 1–5.

[29] Wu W.-Q., Xu Y.-F., Rao H.-S., Su C.-Y., Kuang D.-B. Multi-stack integration of three-dimensional hyperbranched anatase titania architectures for high-efficiency dye-sensitized solar cells. Journal of the American Chemical Society. 2014; 136: 6437–6445.

[30] De Marco L., Manca M., Giannuzzi R., Belviso M.R., Cozzoli P.D., Gigli G. Shape-tailored TiO_2 nanocrystals with synergic peculiarities as building blocks for highly efficient multi-stack dye solar cells. Energy & Environmental Science. 2013; 6 (6): 1791–1795.

[31] Liu X., Guo M., Lin J., Chen X., Huang H. Design of multi-layered TiO_2 nanotube/nanoparticle hybrid structure for enhanced efficiency in dye-sensitized solar cells. RSC Advances. 2014; 4 (85): 45180–45184.

[32] Colodrero S., Mihi A., Häggman L., Ocana M., Boschloo G., Hagfeldt A., et al. Porous one-dimensional photonic crystals improve the power-conversion efficiency of dye-sensitized solar cells. Advanced Materials. 2009; 21 (7): 764–770.

[33] Ok M.-R., Ghosh R., Brennaman M.K., Lopez R., Meyer T.J., Samulski E.T. Surface patterning of mesoporous niobium oxide films for solar energy conversion. ACS Applied Materials & Interfaces. 2013; 5 (8): 3469–3474.

[34] Guldin S., Hüttner S., Kolle M., Welland M., Müller-Buschbaum P., Friend R., et al. Dye-sensitized solar cell based on a three-dimensional photonic crystal. Nano Letters. 2010; 10: 2303–2309.

[35] Chen J.I., von Freymann G., Kitaev V., Ozin G.A. Effect of disorder on the optically amplified photocatalytic efficiency of titania inverse opals. Journal of the American Chemical Society. 2007; 129 (5): 1196–1202.

[36] Lee S.-H ...., Abrams N.M., Hoertz P.G., Barber G.D., Halaoui L.I., Mallouk T.E. Coupling of titania inverse opals to nanocrystalline titania layers in dye-sensitized solar cells. The Journal of Physical Chemistry B. 2008; 112 (46): 14415–14421.

[37] Masuda H., Yamada M., Matsumoto F., Yokoyama S., Mashiko S., Nakao M., et al. Lasing from two-dimensional photonic crystals using anodic porous alumina. Advanced Materials. 2006; 18 (2): 213–216.

[38] Ryu S., Park J., Oh J., Long D., Kwon K., Kim Y., et al. Analysis of improved efficiency of InGaN light-emitting diode with bottom photonic crystal fabricated by anodized aluminum oxide. Advanced Functional Materials. 2009; 19 (10): 1650–1655.

[39] Chen B., Lu K. Influence of patterned concave depth and surface curvature on anodization of titania nanotubes and alumina nanopores. Langmuir. 2011; 27 (19): 12179–12185.

[40] Lin J., Chen X. Synthesis of high-aspect-ratio, top-open and ultraflat-surface TiO_2 nanotubes through double-layered configuration. Physica Status Solidi (RRL)-Rapid Research Letters. 2012; 6 (1): 28–30.

[41] Lee W., Scholz R., Gösele U. A continuous process for structurally well-defined Al_2O_3 nanotubes based on pulse anodization of aluminum. Nano Letters. 2008; 8 (8): 2155–2160.

[42] Lee W., Schwirn K., Steinhart M., Pippel E., Scholz R., Gösele U. Structural engineering of nanoporous anodic aluminium oxide by pulse anodization of aluminium. Nature Nanotechnology. 2008; 3 (4): 234–239.

[43] Wang B., Fei G., Wang M., Kong M., Zhang L. Preparation of photonic crystals made of air pores in anodic alumina. Nanotechnology. 2007; 18 (36): 365601.

[44] Kim D., Ghicov A., Albu S.P., Schmuki P. Bamboo-type TiO_2 nanotubes: Improved conversion efficiency in dye-sensitized solar cells. Journal of the American Chemical Society. 2008; 130 (49): 16454–16455.

[45] Lin J., Liu K., Chen X. Synthesis of periodically structured titania nanotube films and their potential for photonic applications. Small. 2011; 7 (13): 1784–1789.

[46] Yip C.-T., Huang H.T., Zhou L.M., Xie K.Y., Wang Y., Feng T.H., et al. Direct and seamless coupling of TiO_2 nanotube photonic crystal to dye-sensitized solar cell: A single-step approach. Advanced Materials. 2011; 23 (47): 5624–5628.

[47] Guo M., Xie K.Y., Lin J., Yong Z.H., Yip C.-T., Zhou L.M., et al. Design and coupling of multifunctional TiO_2 nanotube photonic crystal to nanocrystalline titania layer as semitransparent photoanode for dye-sensitized solar cell. Energy & Environmental Science. 2012; 5 (12): 9881–9888.

[48] Kuang D.B., Brillet J., Chen P., Takata M., Uchida S., Miura H., et al. Application of highly ordered TiO_2 nanotube arrays in flexible dye-sensitized solar cells. ACS Nano. 2008; 2 (6): 1113–1116.

[49] Shankar K., Bandara J., Paulose M., Wietasch H., Varghese O.K., Mor G.K., et al. Highly efficient solar cells using TiO_2 nanotube arrays sensitized with a donor-antenna dye. Nano Letters. 2008; 8 (6): 1654–1659.

[50] Richter C., Schmuttenmaer C.A. Exciton-like trap states limit electron mobility in TiO_2 nanotubes. Nature Nanotechnology. 2010; 5 (11): 769–772.

[51] Jennings J.R., Ghicov A., Peter L.M., Schmuki P., Walker A.B. Dye-sensitized solar cells based on oriented TiO_2 nanotube arrays: Transport, trapping, and transfer of electrons. Journal of the American Chemical Society. 2008; 130 (40): 13364–13372.

[52] Zhu K., Neale N.R., Halverson A.F., Kim J.Y., Frank A.J. Effects of annealing temperature on the charge-collection and light-harvesting properties of TiO_2 nanotube-based dye-sensitized solar cells. The Journal of Physical Chemistry C. 2010; 114 (32): 13433–13441.

[53] Liu L.J., Chan J., Sham T.K. Calcination-induced phase transformation and accompanying optical luminescence of TiO_2 nanotubes: An X-ray absorption near-edge structures and X-ray excited optical luminescence study. The Journal of Physical Chemistry C. 2010; 114 (49): 21353–21359.

[54] Varghese O.K., Gong D.W., Paulose M., Grimes C.A., Dickey E.C. Crystallization and high-temperature structural stability of titanium oxide nanotube arrays. Journal of Materials Research. 2003; 18 (1): 156–165.

[55] Allam N.K., Grimes C.A. Effect of rapid infrared annealing on the photoelectrochemical properties of anodically fabricated TiO_2 nanotube arrays. The Journal of Physical Chemistry C. 2009; 113 (19): 7996–7999.

[56] Ma Q., Liu S.J. Significantly enhanced structural and thermal stability of anodized anatase nanotube arrays induced by tensile strain. Electrochimica Acta. 2011; 56 (22): 7596–7601.

[57] Wang J., Zhao L., Lin V.S.Y., Lin Z.Q. Formation of various TiO_2 nanostructures from electrochemically anodized titanium. Journal of Materials Chemistry. 2009; 19 (22): 3682–3687.

[58] Fang D., Luo Z.P., Huang K.L., Lagoudas D.C. Effect of heat treatment on morphology, crystalline structure and photocatalysis properties of TiO_2 nanotubes on Ti substrate and freestanding membrane. Applied Surface Science. 2011; 257 (15): 6451–6461.

[59] Lin J., Guo M., Yip C.T., Lu W., Zhang G., Liu X., et al. High temperature crystallization of free-standing anatase TiO_2 nanotube membranes for high efficiency dye-sensitized solar cells. Advanced Functional Materials. 2013; 23 (47): 5952–5960.

[60] Zhu S., Liu X., Lin J., Chen X. Low temperature transferring of anodized TiO 2 nanotube-array onto a flexible substrate for dye-sensitized solar cells. Optical Materials Express. 2015; 5 (12): 2754–2760.

[61] Park J., Bauer S., von der Mark K., Schmuki P. Nanosize and vitality: TiO_2 nanotube diameter directs cell fate. Nano Letters. 2007; 7 (6): 1686–1691.

[62] Liu X., Lin J., Chen X. Synthesis of long TiO_2 nanotube arrays with a small diameter for efficient dye-sensitized solar cells. RSC Advances. 2013; 3 (15): 4885–4889.

[63] Lin J., Liu X., Guo M., Lu W., Zhang G., Zhou L., et al. A facile route to fabricate an anodic TiO_2 nanotube-nanoparticle hybrid structure for high efficiency dye-sensitized solar cells. Nanoscale. 2012; 4 (16): 5148–5153.

[64] Albu S.P., Ghicov A., Aldabergenova S., Drechsel P., LeClere D., Thompson G.E., et al. Formation of double-walled TiO_2 nanotubes and robust anatase membranes. Advanced Materials. 2008; 20 (21): 4135–4139.

[65] Wang D.A., Liu L.F., Zhang F.X., Tao K., Pippel E., Domen K. Spontaneous phase and morphology transformations of anodized titania nanotubes induced by water at room temperature. Nano Letters. 2011; 11 (9): 3649–3655.

[66] Liao Y.L., Que W.X., Zhong P., Zhang J., He Y.C. A facile method to crystallize amorphous anodized TiO_2 nanotubes at low temperature. ACS Applied Materials & Interfaces. 2011; 3 (7): 2800–2804.

[67] Pan X., Chen C.H., Zhu K., Fan Z.Y. TiO_2 nanotubes infiltrated with nanoparticles for dye sensitized solar cells. Nanotechnology. 2011; 22 (23): 235402.

[68] Wang S.H., Zhang J.B., Chen S., Yang H.T., Lin Y., Xiao X.R., et al. Conversion enhancement of flexible dye-sensitized solar cells based on TiO_2 nanotube arrays with TiO_2 nanoparticles by electrophoretic deposition. Electrochimica Acta. 2011; 56 (17): 6184–6188.

IntechOpen